Particle & Particle Systems Characterization
www.particle-journal.com

Highly Luminescent Carbon-Nanoparticle-Based Materials: Factors Influencing Photoluminescence Quantum Yield

Songnan Qu, Dezhen Shen, Xingyuan Liu,* Pengtao Jing, Ligong Zhang, Wenyu Ji, Haifeng Zhao, Xiwu Fan, and Hong Zhang**

Unravelling the factors influencing photoluminescence (PL) quantum yield of the carbon nanoparticles (CNPs) is the prerequisite for preparing highly luminescent CNP-based materials. In this work, an easy and effective method is reported for preparing highly luminescent CNP-based materials. Water-soluble luminescent CNPs (CNP-Cs) with large size distribution (1–60 nm) with PL quantum yields of 22% are synthesized through a microwave pyrolysis approach. Energy transfer (ET) is confirmed to occur from small size CNPs (CNP-Ss:1-7 nm, blue emitters) to large size CNPs (CNP-Ls:10–60 nm, green emitters). Further centrifugally separating CNP-Cs resulted in an enhancement of the PL quantum yield up to 39% of CNP-Ss aqueous solution. The PL quantum yield of CNP-Ss could even be further improved in high-viscosity solvents. PL quantum yield higher than 90% is achieved in films of commercial glue water embedded with the CNP-Ss at embedding ratio lower than 3 wt%. By contrast, the yield is greatly decreased in the CNP-C-embedding films with embedding ratio higher than 1 wt%, which is due to self-absorption, as well as enhanced ET between CNP-Ss and CNP-Ls. High-viscosity solvents and polymer matrix are proposed to act as surface passivation reagents to enhance PL quantum yield of CNPs.

1. Introduction

Carbon is hardly considered a luminescent material, but carbon nanoparticles (CNPs) could be made to brightly luminesce.[1] Intensive studies have been carried out on luminescent CNPs in recent years due to their exceptional advantages, such as high abundance, chemical inertness, high resistance to photobleaching, excellent biocompatibility, green synthesis, low cost as well as low toxicity, which make the material promising candidates for bioimaging,[2] medical diagnosis,[3] fluorescent probes,[4] and optoelectronic devices.[5]

Prof. S. Qu, Prof. D. Shen, Prof. X. Liu, Dr. P. Jing, Prof. L. Zhang, Dr. W. Ji, Dr. H. Zhao, Prof. X. Fan
State Key Laboratory of Luminescence and Applications
Changchun Institute of Optics
Fine Mechanics and Physics
Chinese Academy of Sciences
Changchun 130033, PR China
E-mail: shendz@ciomp.ac.cn; liuxy@ciomp.ac.cn
Prof. H. Zhang
Van't Hoff Institute for Molecular Sciences
University of Amsterdam
Science Park 904
1098 XH, Amsterdam, The Netherlands
E-mail: H.Zhang@uva.nl

DOI: 10.1002/ppsc.201400055

High photoluminescence (PL) quantum yield is a primary property of CNPs, which relates directly to their applications. The quantum yields of unfunctionalized CNPs are often less than 10%. Great effort has been taken to improve the PL quantum yield of CNPs through various chemistry methods.[1] For example, Yang and co-workers[6] reported a facile and high-output method for the fabrication of CNPs with a PL quantum yield as high as 80% via hydrothermal method. Liu and co-workers[7] reported organic–inorganic hybrid functional CNP Gel Glasses, in which PL quantum yield up to 88% was achieved at low CNP loading fraction (0.01 wt%). On the other hand, enhancement of PL quantum yield of CNPs was also reported through physical methods. Sun and co-workers[8] reported that CNPs with PL quantum yield of 55–60% can be obtained through column chromatography from CNP mixture with PL quantum yield of 16–20%. Colón and co-workers[9] reported that CNPs with PL quantum yield of 6–7% can be acquired simply through high-resolution anion-exchange (AE) high-performance liquid chromatography (HPLC) fraction from the CNP mixture of 1% PL quantum yield. It should be noted that the reported purified CNPs with improved PL quantum yields exhibit much weaker excitation-wavelength-dependent emissions than the crude CNPs, indicating the crude CNPs were mixtures of different luminescent species with different PL quantum yields and different emission wavelengths. However, the underlying mechanism is still vague. To date, CNP luminescent process has been investigated predominantly in dilute solutions and only few reports in CNP-embedded polymer films,[10] CNPs/organic, or inorganic heterostructures.[5b,11] As most of the envisioned applications or devices are not based on single-particle CNPs or their solutions with the exception of biological applications, it is desired to prepare highly luminescent CNP-based solid-state materials and exploit the factors influencing their PL quantum yields. The reported CNP-based solid-state materials with high PL quantum yield were only achieved at low CNP-loading fraction.[7] In high-CNP-content systems, self-absorption or energy transfer (ET) would occur, unfavorable to high luminescence. To the best of our knowledge, no report has appeared until now on ET behavior between CNPs, although it is very important for preparing highly luminescent CNP-based materials and CNP-based optoelectronic devices.

Previously, we reported an easy, economic, and green one-step microwave synthesis for water-soluble luminescent CNPs from citric acid and urea, which could be used as a new type of biocompatible fluorescent ink, ratiometric fluorescent nanosensors, and laser material.[12] Here, we report an easy and effective method for preparing highly luminescent CNP-based materials. Water-soluble luminescent CNPs (CNP-Cs) with large size distribution (1–60 nm) with PL quantum yields of 22% were synthesized through microwave pyrolysis approach. ET was observed to occur from small size CNPs (CNP-Ss:1–7 nm, blue emitters) to large size CNPs (CNP-Ls:10–60 nm, green emitters). Separating CNP-Ls through centrifugal process improved the PL quantum yield to 39% in CNP-Ss aqueous solution. The PL quantum yield of CNP-Ss was further enhanced in high-viscosity solvents. It is exciting to find that PL quantum yield higher than 90% was achieved in films of commercial glue water embedded with the CNP-Ss at embedding ratio lower than 3 wt%, which is the highest value recorded for CNP-based materials. PL quantum yields higher than 30% was achieved in the CNP-S-embedded films at relatively high embedding ratio (≈7.4 wt%), which was greatly decreased in the CNP-C-embedding films at embedding ratios higher 1 wt%, due to self-absorption and enhanced ET between CNP-Ss and CNP-Ls.

2. Results and Discussion

2.1. Preparation of CNPs

Citric acid is widely used as carbon source in preparing CNPs.[1] CNPs prepared from citric acid without adding any other compounds in microwave synthesis showed weak blue luminescence with a PL quantum yield of 3%, similar to previous report.[12c,13] On the other hand, it was reported that the doped nitrogen can improve the emission of the CNPs by inducing an upward shift of the Fermi level and electrons in the conduction band.[14] Based on this understanding, we prepared CNPs from citric acid and ammonia water in microwave synthesis aiming at enhancing PL quantum yield, in which ammonia water, which can be easily disposed off, was used as a nitrogen doping source. Citric acid (3 g) was firstly added to ammonia water (25% ammonia by mass, 20 mL) to form a transparent solution. The solution was heated in a domestic 650 W microwave oven for 5–6 min, during which the solution changed from a colorless to brown and finally dark-brown liquid, indicating the formation of CNPs. After drying in an oven at 60 °C, the products were transferred to a vacuum oven and heated at 60 °C for 2 h. The crude CNPs (CNP-Cs) were diluted in aqueous solution. A possible growth mechanism of the CNP-Cs is illustrated in **Scheme 1**.

2.2. Characterization of CNPs

The morphologies of the CNP-Cs were characterized using transmission electron microscopy (TEM) and atomic force microscopy (AFM). Drops of a CNP-C dilute aqueous solution were deposited on a carbon-coated copper grid for TEM measurements and on silicon substrates for AFM measurements, respectively. The TEM images (**Figure 1**a,b) and AFM image (**Figure 2**b, Figure S2, Supporting Information) illustrate that the CNP-Cs are spherical and well dispersed, ranging from 1 to 60 nm. The high-resolution TEM (HRTEM) image (Figure 1b) of small-sized CNPs reveals their lattice fringes of 0.21, 0.25, 0.27, and 0.31 nm, which are consistent with the (102), (100), (020), and (002) lattice planes of graphitic carbon.[1] The Raman spectra of the CNP-Cs (Figure S5, Supporting Information) display two broad peaks at 1361 and 1577 cm^{-1}, which are attributed to the D-band (sp^3) and G-band (sp^2), respectively. The D-band is associated with vibrations of carbon atoms with dangling bonds in the termination planes of disordered graphite or glassy carbon. The G-band corresponds to the E_{2g} mode of graphite and is related to the sp^2-bonded carbon atom vibrations in a 2D hexagonal lattice.[15] The relative intensity of the "disordered" D-band and crystalline G-band (I_D/I_G) for the CNPs is around 0.93, indicating a similar structure to graphite. The X-ray photoelectron spectroscopy (XPS) spectrum of the CNP-Cs (Figure 1c) has three peaks at 284.0, 400.0, and 530.6 eV, which are attributed to C_{1s}, N_{1s}, and O_{1s}, respectively. The C_{1s} spectrum (Figure 1d) shows four peaks at 284.6, 285.7, 286.6, and 288.3 eV, corresponding to sp^2 C, C—N, C—O and C=N/C=O, respectively.[16] The N_{1s} spectrum (Figure 1e) has three peaks at 399.4 (C—N—C), 400.2 (N—(C)3), and 401.4 eV (N—H), respectively, confirming the doping of N atoms and amide-N.[17] N atoms doping was further evidenced by the appearance of the C=N bond at 1562 cm^{-1} in the FT-IR spectrum (Figure 1f). The two peaks at 532.0 and 533.7 eV of O_{1s} spectrum (Figure S6, Supporting Information) are attributed to C=O and C—OH/C—O—C groups, respectively. The surface functional groups of the CNP-Cs were detected by FT-IR (Figure 1f). Broad absorption bands at 3050–3552 cm^{-1} are assigned to ν(N—H) and ν(O—H), whereas those at 1640–1780 cm^{-1} are assigned to

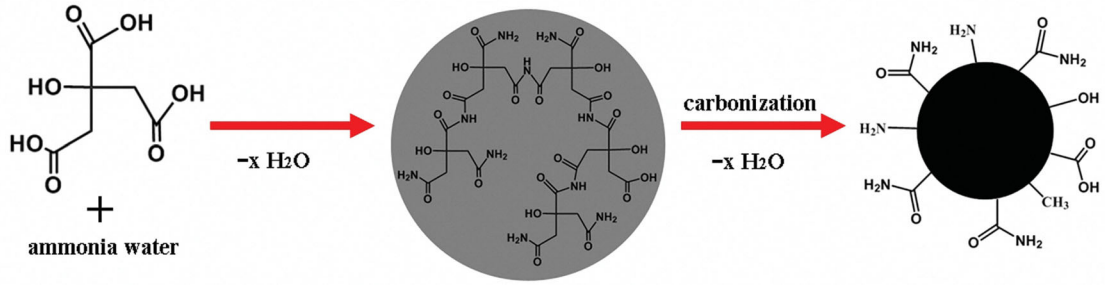

Scheme 1. A possible growth mechanism of the CNP-Cs.

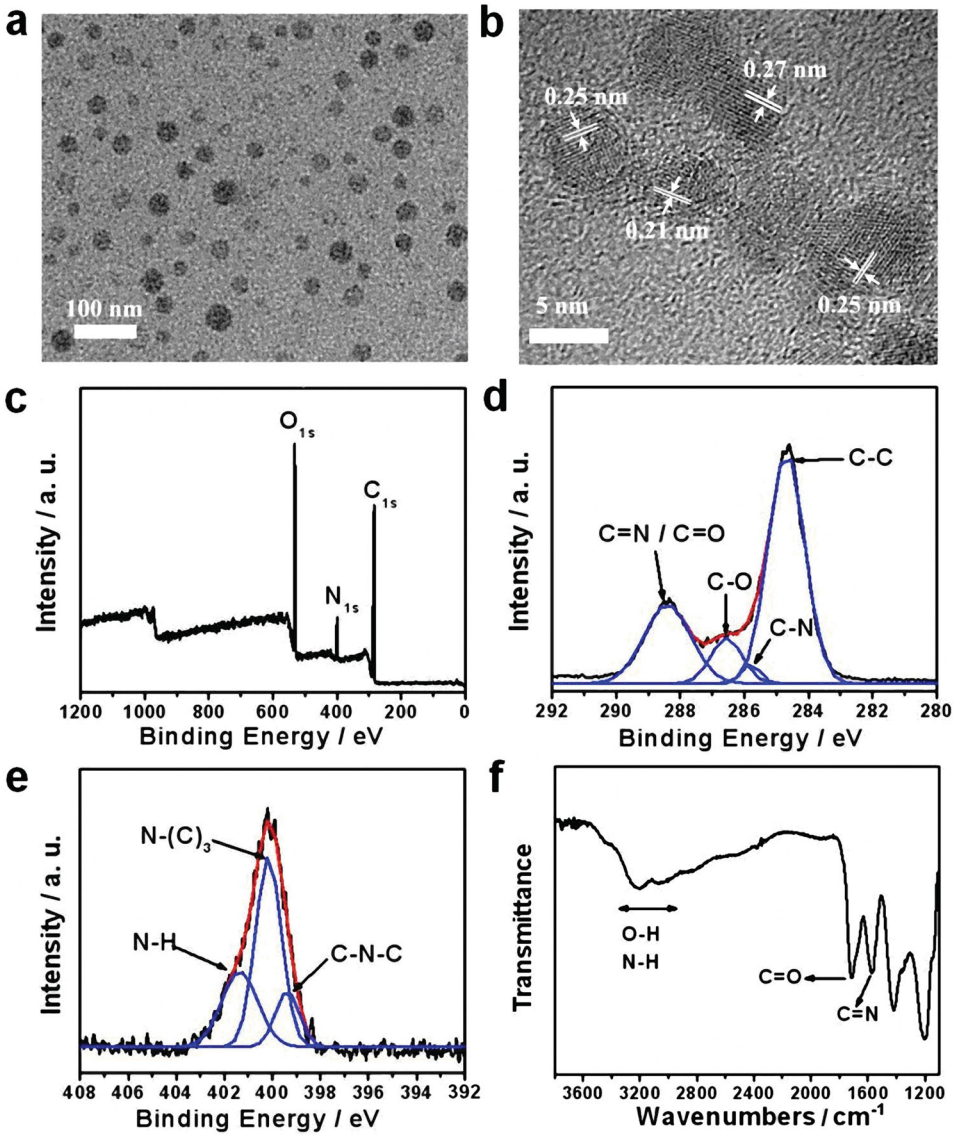

Figure 1. a) TEM image of CNP-Cs and b) HRTEM image of small sized CNPs. c) XPS, d) C_{1s} and e) N_{1s} spectra, f) FT-IR spectrum of the CNP-Cs in the dry state.

ν(C═O). The amino groups appear in the ^{1}H NMR spectrum with N—H signal at 8.5 ppm (Figure S7, Supporting Information). These functional groups improve the hydrophilicity and stability of the CNP-Cs in aqueous systems.

2.3. Optical Properties of CNPs

The CNP-Cs dilute aqueous solution exhibits excitation-wavelength-dependent PL properties (Figure 2a, Figure S8a, Supporting Information). Under 360 nm excitation, the strongest emission with quantum yield of 22% was observed centered at 436 nm (≈2.84 eV). When the excitation wavelength changes from 360 nm to 480 nm, the emission decrease in intensity and red-shift from 440 to 558 nm. Another local maximum emission centered at 545 nm (≈2.28 eV) was observed under blue light excitation (Figure 2a). When the CNP-Cs aqueous solution centrifuged at 16 000 r min^{-1} for 20 min, precipitates were observed. From AFM, it could be determined that the precipitates were large size CNPs (CNP-Ls) from 10 to 60 nm in height (Figure 2d, Figure S3, Supporting Information). The strongest emission centered at 545 nm (≈2.28 eV) of CNP-Ls dilute aqueous solution was observed under 460 nm excitation (Figure 2c, Figure S8b, Supporting Information) with quantum yield of 13%. Most of the large size CNPs could be separated off by centrifuging the CNPs ethanol aqueous solutions (ethanol volume concentration: 75%) at 16 000 r min^{-1} for 20 min. The obtained supernate contains predominantly small size CNPs (CNP-Ss) from 1 to 7 nm as evidenced by AFM patterns (Figure 2f; Figure S4, Supporting Information). The CNP-Ss dilute aqueous solution exhibited weaker excitation-wavelength-dependent emission spectrum than CNP-Cs dilute aqueous

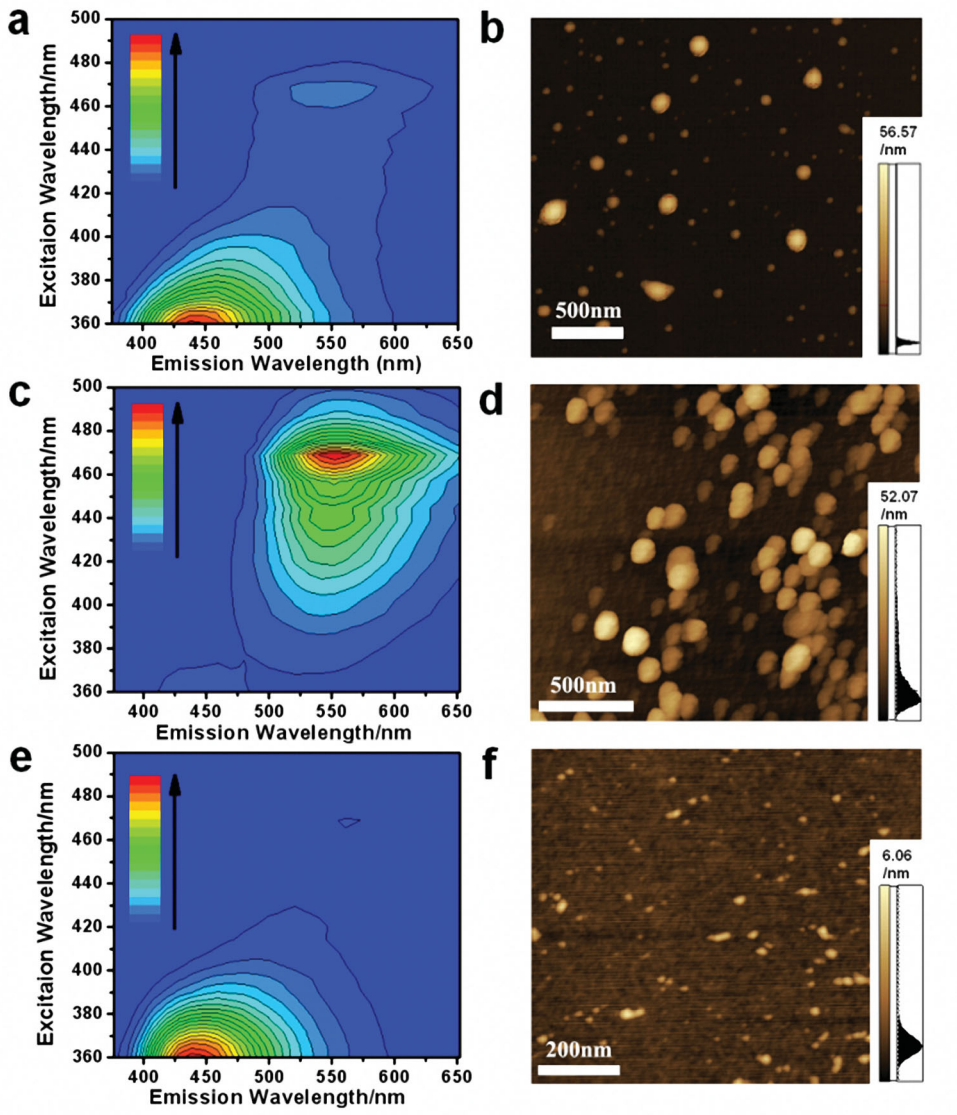

Figure 2. Excitation–emission matrices for a) CNP-Cs, c) CNP-Ls and e) CNP-Ss dilute aqueous solutions (0.1 mg mL^{-1}). AFM images of b) CNP-Cs, d) CNP-Ls, and f) CNP-Ss on silicon substrates.

solution (Figure 2e; Figure S8c, Supporting Information). Under 360 nm excitation, the strongest emission of CNP-Ss dilute aqueous solution is centers at 436 nm (≈2.84 eV) and the quantum yield is 39%. As shown in excitation–emission matrices, the relative luminescence intensity of the green luminescent species of CNP-Ss dilute aqueous solution decreases in comparison with that of CNP-Cs dilute aqueous solution under blue light excitation (Figure 2e). The CNP-Ss dilute aqueous solution exhibits an absorption band peaking at 335 nm (≈3.70 eV), which is typical for aromatic π systems (**Figure 3**a). By contrast, the CNP-Ls dilute aqueous solution has a new absorption band centered at 430 nm (≈2.88 eV), indicating extended π-conjugated structures, which could lead to longer wavelength emission. The fact that the luminescence lifetime of CNP-Ls dilute aqueous solution is shorter than that of CNP-Ss dilute aqueous solution indicates difference in the excited state dynamics (Figure S10, Supporting Information; **Table 1**). It can be concluded that CNP-Ss correspond to the blue luminescent species, while CNP-Ls to the green one. At this stage, the origin of the luminescence of the CNPs is unclear. Considering the obviously absorption bonds, size-dependent absorption and emissions, we propose that the luminescence of the CNPs is attributed to electron-hole recombination (intrinsic state emission).

2.4. Factors Influencing the PL Quantum Yield of CNPs

It can be seen that the bandgap of CNP-Ss (≈3.70 eV) is larger than that of CNP-Ls (≈2.88 eV), and the maximum emission band of CNP-Ss (360 nm excitation) overlaps the excitation band of CNP-Ls (monitored at 540 nm) (Figure 3b). Thus, CNP-Ss and CNP-Ls may act as donor and acceptor for ET. Indeed it was observed that efficient luminescence quenching occurs with

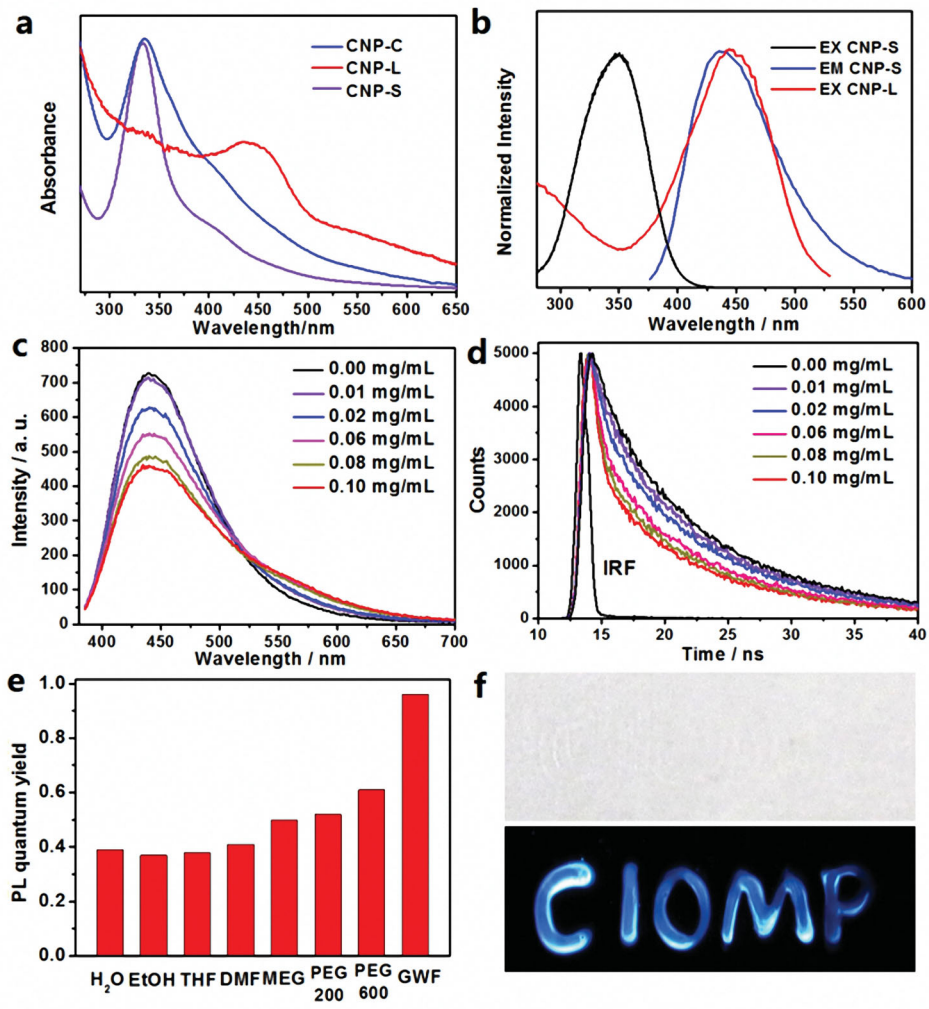

Figure 3. a) UV–Vis absorption spectra of CNP-Cs, CNP-Ls, and CNP-Ss dilute aqueous solutions. b) Excitation spectra of CNP-Ss (monitored at 440 nm) and CNP-Ls (monitored at 540 nm) dilute aqueous solutions (0.1 mg mL^{-1}), and PL spectrum of spectra of CNP-Ss at 360 nm excitation. c) PL spectra and d) time-resolved luminescence decay curves collected at 440 nm for CNP-Ss aqueous solution (0.4 mg mL^{-1}) in the present of different concentrations of CNP-Ls (375 nm excitation). e) PL quantum yields of the CNP-Ss in different solvents (0.1 mg mL^{-1}) (THF: tetrahydrofuran, DMF: dimethyl formamide, MEG: ethylene glycol, PEG200: polyethylene glycol 200, PEG600: polyethylene glycol 600) and polymer matrix (GWF: 0.6 wt% CNP-S-embedded glue water film) (λ_{ex} = 360 nm). f) Optical (top) and fluorescent photographs (bottom) of characters made from CNP-S-embedded glue water on glass substrate upon UV illumination.

luminescence lifetime of CNP-Ss shortening when CNP-Ls were added in aqueous solutions (Figure 3c,d). The luminescence decay curve collected at 440 nm (under 375 nm excitation) for CNP-Ss aqueous solution in the absence of CNP-Ls can be well fitted by biexponential function with average lifetime τ_0 of 9.25 ns. Increasing CNP-Ls concentrations, the luminescence decay curve collected at 440 nm can only be fitted by tri-exponential function and the average lifetime τ decreases (Table S1, Supporting Information). These facts indicate that the enhanced PL quantum yield of CNP-Ss was due to not only separate off less luminescent CNP-Ls but also decrease in ET process between CNP-Ss (donors) and CNP-Ls (acceptors).[18]

Table 1. Optical properties of CNP-Ls and CNP-Ss dilute aqueous solutions.

	λ_{abs} [nm]	$\lambda_{em,max}$ [nm]	τ [ns]	χ^2	ΦF
CNP-S	335	436	3.2 (6.3%) 10.1 (93.7%)	0.9	0.39
CNP-L	430	545	7.2	1.2	0.13

It is interesting to note that PL quantum yield of CNP-Ss is enhanced in high-viscosity solvents (Figure 3e). In CNP-Ss dilute polyethylene glycol (PEG) 600 solution, it is 61% at room temperature. The question raised therefore is: can the PL quantum yield be further enhanced in a higher-viscosity system? To disentangle this speculation, we put the CNPs in solid polymer matrix. The CNP-Cs and CNP-Ss were well dispersed in commercial glue water (main element: polyvinyl alcohol (PVA)). When the CNP-C-embedded and CNP-S-embedded glue water coated on quartz or glass plates and dried at room temperature, high luminescence occurred. As no luminescence

Table 2. PL quantum yields of CNP-C-embedded and CNP-S-embedded films at different embedding ratios.

	0.6 wt%	0.9 wt%	2.8 wt%	3.7 wt%	7.4 wt%
CNP-C-embedded film	0.84	0.43	0.28	0.22	0.16
CNP-S-embedded film	0.96	0.94	0.90	0.46	0.35

was observed from the glue water (solution or dried film) at excitation wavelengths longer than 360 nm, the luminescence originated from the embedded CNPs. Under 360 nm excitation, PL quantum yield higher than 90% could be achieved in CNP-S-embedded film at an embedding ratio lower than 3 wt% with the strongest mission band centered at 425 nm (Figure S9, Supporting Information; **Table 2**). PL quantum yield higher than 30% could be obtained in the CNP-S-embedded films at relatively high embedding ratios (≈7.4 wt%). Luminescence of CNP-Ss-embedded glue water is illustrated in Figure 3f. These results emphasize that CNP-Ss embedded glue water can be used as a new type of luminescent coating.

High PL quantum yield up to 84% could also be achieved in CNP-C-embedded film at low embedding ratio of 0.6 wt% with the strongest mission centered at 425 nm under 360 nm excitation (**Figure 4**a, Table 2). In contrast, the PL quantum yield was greatly decreased in the CNP-C-embedding films at embedding ratio higher than 1 wt%. The PL spectra for 0.6 wt% and 2.8 wt% CNP-C-embedded films are shown in Figure 4a,b. It can be seen that the PL spectra of 2.8 wt% CNP-C-embedded film is broadened and red-shifted under 360 nm excitation, and the relative intensity of the green luminescence species under blue light excitations is increased, comparing with that of 0.6 wt% CNP-C-embedded film. The red-shifted emission might be due to self-absorption in high CNP-Cs embedding ratio. The excitation spectra (normalized at 444 nm) of 0.6 wt%, 2.8 wt%, and 7.4 wt% CNP-C-embedded films (monitored at 540 nm) are shown in Figure 4c. When CNP-Cs embedding ratio increased, 345 nm band was getting higher than the rest bands. Furthermore, the luminescence lifetime at 440 nm of CNP-C-embedded films decreased upon increasing CNP-Cs embedding ratio (Figure 4d). The concentration-dependent luminescence of CNP-C-embedded films indicates the sensitivity of the excited state dynamics on the distance between CNPs. It therefore can be concluded that the decrease of the PL quantum yield of CNP-C-embedded films when CNP-Cs embedding ratios getting higher is due to not only self-absorption but also enhanced ET between CNP-Ss and CNP-Ls. In previous reports, the PL quantum yields for CNPs without surface passivation are very low (<10%). To enhance luminescence, polymers or long-chain molecules were chemically linked on CNPs as surface passivation reagents, which might decrease defect sites (energy dissipative) on the surface of CNPs. In our case, we proposed that high-viscosity solvents and polymer matrix might act as surface passivation reagents to enhance PL quantum yield of CNPs. This method is easy and effective.

3. Conclusion

In summary, we report an easy and effective method for preparing highly luminescent CNP-based materials.

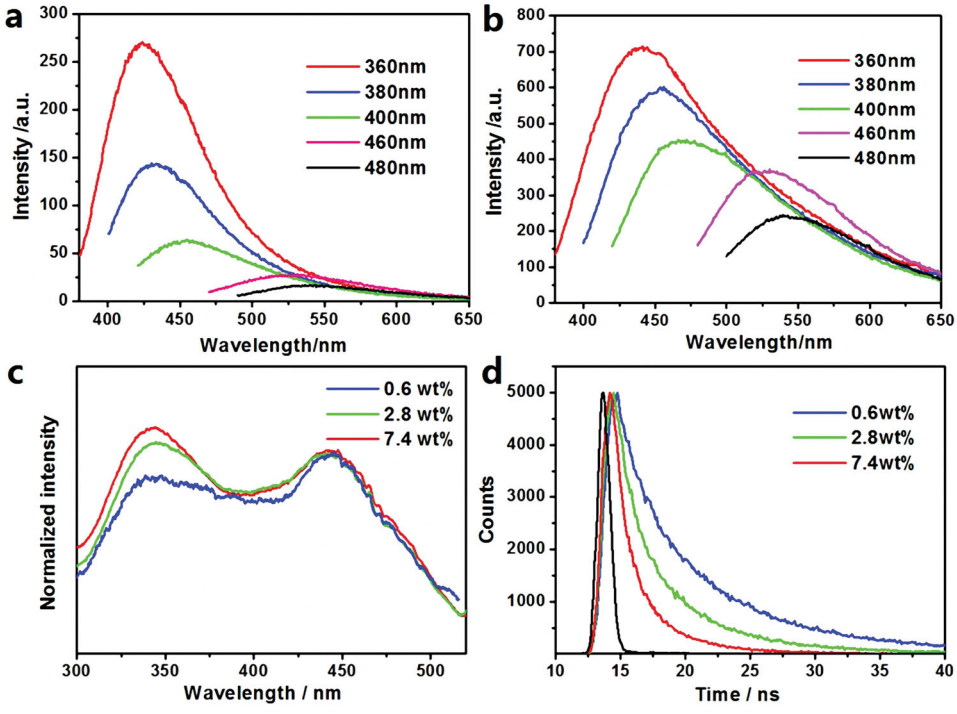

Figure 4. PL spectra of a) 0.6 wt% and b) 2.8 wt% CNP-C-embedded films at different excitation wavelengths. c) Excitation spectra (normalized at 444 nm) for 0.6 wt%, 2.8 wt%, and 7.4 wt% CNP-C-embedded films (monitored at 540 nm). d) Time-resolved luminescence decay curves collected at 440 nm for 0.6 wt%, 2.8 wt%, and 7.4 wt% CNP-C-embedded films.

Water-soluble luminescent CNPs (CNP-Cs) with large size distribution (1–60 nm) with PL quantum yields of 22% were synthesized through a microwave pyrolysis approach. ET was confirmed to occur from small size CNPs (CNP-Ss: 1–7 nm, blue emitters) to large size CNPs (CNP-Ls: 10–60 nm, green emitters). Centrifugally separating CNP-Ls enhanced the PL quantum yield to 39% in CNP-Ss aqueous solution. The PL quantum yield of CNP-Ss was further enhanced in high-viscosity solvents. PL quantum yields higher than 90% was also achieved in films of commercial glue water embedded with the CNP-Ss at embedding ratio lower than 3 wt%. PL quantum yield higher than 30% was obtained in the CNP-S-embedded films at relatively high embedding ratios (≈7.4 wt%), which was greatly decreased in the CNP-C-embedding films at embedding ratios higher 1 wt% due to not only self-absorption but also enhanced ET between CNP-Ss and CNP-Ls. High-viscosity solvents and polymer matrix were proposed to play as surface passivation reagents to enhance PL quantum yield of CNPs. Our efforts shine a light on unravelling the factors influencing PL quantum yield of CNP-based materials, and bring a hope and offer a method in preparing highly luminescent CNP-based materials towards 100% PL quantum yield.

4. Experimental Section

Characterizations: TEM observations were performed on a FEI Tecnai-G2-F20 TEM at 200 kV. AFM measurements were performed on a SA400HV with a SPI3800N controller, Seiko Instruments Industry, Co. Ltd.. Raman spectra were collected using an UV-lamp spectroscope with a 300 mW Ar+ laser (488 nm) as the excitation source. XPS analyzes were measured on an ESCALAB MK II X-ray photoelectron spectrometer using Mg as the exciting source. 1H NMR spectra were recorded with a Varian-300 EX spectrometer. FT-IR spectra were recorded using a Perkin–Elmer spectrometer (Spectrum One B). PL spectra were collected using FLS920 spectrometer and Hitachi Fluorescence spectrophotometer-F-7000. UV–vis absorption spectra were recorded on a Shimadzu UV-3101PC spectrophotometer. PL quantum yields were obtained in a calibrated integrating sphere using a FLS920 spectrometer. Luminescence lifetimes were measured using FLS920 time-corrected single photon counting (TCSPC) system. X-ray diffraction (XRD) was performed with a Bruker Advance D8 X-ray diffractometer. The water used in all experiments was purified through a Millipore system.

Supporting Information

Supporting Information is available from the Wiley Online Library or from the author.

Acknowledgements

This work is supported by the CAS Innovation Program, National Science Foundation of China No. 51103144, 11204298, 61205025, 61274126, Jilin Province Science and Technology Research Project No. 20140101060JC and Project supported by State Key Laboratory of Luminescence and Applications.

Received: March 17, 2014
Revised: April 12, 2014
Published online: June 13, 2014

[1] a) S. N. Baker, G. A. Baker, *Angew. Chem. Int. Ed.* **2010**, *49*, 6726; b) J. C. G. Esteves da Silva, H. M. R. Goncalves, *Trends Anal. Chem.* **2011**, *30*, 1327; c) H. Li, Z. Kang, Y. Liu, S. T. Lee, *J. Mater. Chem.* **2012**, *22*, 24230.

[2] a) L. Cao, X. Wang, M. J. Meziani, F. Lu, H. Wang, P. G. Luo, Y. Lin, B. A. Harruff, L. M. Veca, D. Murray, S. Y. Xie, Y. P. Sun, *J. Am. Chem. Soc.* **2007**, *129*, 11318; b) F. Wang, Z. Xie, H. Zhang, C. Y. Liu, Y. G. Zhang, *Adv. Funct. Mater.* **2011**, *21*, 1027; c) Y. Xu, M. Wu, Y. Liu, X. Z. Feng, X. B. Yin, X. W. He, Y. K. Zhang, *Chem. Eur. J.* **2013**, *19*, 2276; d) Y. Song, D. Feng, W. Shi, X. Li, H. Ma, *Talanta* **2013**, *116*, 237.

[3] a) L. Cao, S. Sahu, P. Anilkumar, C. E. Bunker, J. Xu, K. A. S. Fernando, P. Wang, E. A. Guliants, K. N. Tackett, Y. P. Sun, *J. Am. Chem. Soc.* **2011**, *133*, 4754; b) H. T. Li, X. He, Z. Kang, H. Huang, Y. Liu, J. Liu, S. Lian, A. C. H. Tsang, X. Yang, S. T. Lee, *Angew. Chem. Int. Ed.* **2010**, *49*, 4430; c) C. H. Lee, R. Rajendran, M.-S. Jeong, H. Y. Ko, J. Y. Joo, S. Cho, Y. W. Chang, S. Kim, *Chem. Commun.* **2013**, *49*, 6543.

[4] a) H. X. Zhao, L. Q. Liu, Z. D. Liu, Y. Wang, X. J. Zhao, C. Z. Huang, *Chem. Commun.* **2011**, *47*, 2604; b) Wei, C. Xu, J. Ren, B. Xu, X. Qu, *Chem. Commun.* **2012**, *48*, 1284; c) L. Zhou, Y. Lin, Z. Huang, J. Ren, X. Qu, *Chem. Commun.* **2012**, *48*, 1147; d) S. Liu, J. Tian, L. Wang, Y. Zhang, X. Qin, Y. Luo, A. M. Asiri, A. O. Al-Youbi, X. Sun, *Adv. Mater.* **2012**, *24*, 2037; e) M. J. Krysmann, A. Kelarakis, P. Dallas, E. P. Giannelis, *J. Am. Chem. Soc.* **2012**, *134*, 747; f) J. M. Liu, L. Lin, X. X. Wang, S. L. Lin, W. L. Cai, L. H. Zhang, Z. Y. Zheng, *Analyst* **2012**, *137*, 2637; g) W. Shi, X. Li, H. Ma, *Angew. Chem. Int. Ed.* **2012**, *51*, 6432; h) A. Zhu, Q. Qu, X. Shao, B. Kong, Y. Tian, *Angew. Chem. Int. Ed.* **2012**, *51*, 7185.

[5] a) X. Yan, X. Cui, B. Li, L. Li, *Nano Lett.* **2010**, *10*, 1869; b) Y. Li, Y. Hu, Y. Zhao, G. Shi, L. Deng, Y. Hou, L. Qu, *Adv. Mater.* **2011**, *23*, 776; c) F. Wang, Y. Chen, C. Liu, D. Ma, *Chem. Commun.* **2011**, *47*, 3502; d) X. Zhang, Y. Zhang, Y. Wang, S. Kalytchuk, S. V. Kershaw, Y. Wang, P. Wang, T. Zhang, Y. Zhao, H. Zhang, T. Cui, Y. Wang, J. Zhao, W. W. Yu, A. L. Rogach, *ACS Nano* **2013**, *7*, 11234.

[6] S. Zhu, Q. Meng, L. Wang, J. Zhang, Y. Song, H. Jin, K. Zhang, H. Sun, H. Wang, B. Yang, *Angew. Chem. Int. Ed.* **2013**, *52*, 3953.

[7] Z. Xie, F. Wang, C. Liu, *Adv. Mater.* **2012**, *24*, 17162290.

[8] X. Wang, L. Cao, S. T. Yang, F. Lu, M. J. Meziani, L. Tian, K. W. Sun, M. A. Bloodgood, Y. P. Sun, *Angew. Chem. Int. Ed.* **2010**, *49*, 53102290.

[9] J. C. Vinci, I. M. Ferrer, S. J. Seedhouse, A. K. Bourdon, J. M. Reynard, B. A. Foster, F. V. Bright, L. A. Colón, *J. Phys. Chem. Lett.* **2013**, *4*, 239.

[10] a) P. Zhang, W. Li, X. Zhai, C. Liu, L. Dai, W. Liu, *Chem. Commun.* **2012**, *48*, 10431; b) Y. Deng, D. Zhao, X. Chen, F. Wang, H. Song, D. Shen, *Chem. Commun.* **2013**, *49*, 5751; c) W. Kwon, S. Do, J. Lee, S. Hwang, J. K. Kim, S.-W. Rhee, *Chem. Mater.* **2013**, *25*, 1893.

[11] a) Y. Li, B.-P. Zhang, J.-X. Zhao, Z.-H. Ge, X.-K. Zhao, L. Zou, *Appl. Surf. Sci.* **2013**, *279*, 367; b) X. Zhang, F. Wang, H. Huang, H. Li, X. Han, Y. Liu, Z. Kang, *Nanoscale* **2013**, *5*, 2274; c) S. Mondal, T. Das, P. Ghosh, A. Maity, A. Mallick, P. Purkayastha, *Chem. Commun.* **2013**, *49*, 7638; d) X. Wang, L. Cao, F. Lu, M. J. Meziani, H. Li, G. Qi, B. Zhou, B. A. Harruff, F. Kermarrec, Y.-P. Sun, *Chem. Commun.* **2009**, 3774.

[12] a) S. Qu, X. Wang, Q. Lu, X. Liu, L. Wang, *Angew. Chem. Int. Ed.* **2012**, *51*, 12215; b) S. Qu, H. Chen, X. Zheng, J. Cao, X. Liu, *Nanoscale* **2013**, *5*, 5514; c) S. Qu, X. Liu, X. Guo, M. Chu, L. Zhang, D. Shen, *Adv. Funct. Mater.* **2014**, DOI: 10.1002/adfm.201303352.

[13] X. Zhai, P. Zhang, C. Liu, T. Bai, W. Li, L. Dai, W. Liu, *Chem. Commun.* **2012**, *48*, 7995.

[14] P. Ayala, R. Arenal, A. Loiseau, A. Rubio, T. Pichler, *Rev. Mod. Phys.* **2010**, *82*, 1843.
[15] R. Liu, D. Wu, S. Liu, K. Koynov, W. Knoll, Q. Li, *Angew. Chem. Int. Ed.* **2009**, *48*, 4598.
[16] L.-L. Li, J. Ji, R. Fei, C.-Z. Wang, Q. Lu, J.-R. Zhang, L.-P. Jiang, J.-J. Zhu, *Adv. Funct. Mater.* **2012**, *22*, 2971.
[17] S. Fleutot, J.-C. Dupin, G. Renaudin, H. Martinez, *Phys. Chem. Chem. Phys.* **2011**, *13*, 17564.
[18] a) B. Valeur, *Molecular Fluorescence: Principles and Applications*, Wiley-VCH, Weinheim, Germany **2001**; b) J. R. Lakowicz, *Principles of Fluorescence Spectroscopy*, 3rd edn, Springer, New York **2006**.